Enhancing open-loop control of MEMS using linear electrostatic levitation actuators

Mohammad Mousavi
Mechanical Engineering Department
Binghamton University
Binghamton, New York, USA
Email: smousav1@binghamton.edu

Mohammad Alzgool
Mechanical Engineering Department
Binghamton University
Binghamton, New York, USA
Email: malzgoo1@binghamton.edu

Shahrzad Towfighian
Mechanical Engineering Department
Binghamton University
Binghamton, New York, USA
Email: stowfigh@binghamton.edu

2021 IEEE Sensors | 978-1-7281-9501-8/21/$31.00 ©2021 IEEE | DOI: 10.1109/SENSORS47087.2021.9639780

***Abstract*—MEMS electrostatic actuators are used in optical applications because of their small size and quick response. However, nonlinearities of electrostatic force, long settling-time and small range of motion significantly hampers their performance. Adding electrostatic levitation to MEMS parallel-plate mechanism, we achieved a wide linear operation region away from the center electrode. Because of linearity, command-shaping becomes an easy and effective method to decrease the settling-time and overshoot. Compared to the conventional parallel-plate electrodes, we have shown a considerable increase in the travel range of levitating electrodes using double-step command signals.**

***Keywords*—MEMS, Command-shaping, open-loop control, electrostatic levitation, fringe field**

I. Introduction

The control of mechanical systems such as micro-electromechanical system (MEMS) is a crucial mission nowadays. A great deal of financial supports is dedicated to enhancement of the performance of MEMS systems [1]–[3]. In industrial applications, the hardware specifications are limited because of the complex circuits and electronics and therefore, feedback control of MEMS is not still very popular. Considering high quality factor MEMS devices, static displacement and scanning applications are widely used [4]–[11]. Using a single pulse drive, switching between static displacement and scanning mode takes a considerable time because of the undesired oscillations should fade, which limits the system performance. Researchers have shown how command-shaping techniques allow for activating and deactivating a specific mode of the system. Static displacement and scanning is used without suffering from the slow response time. In [6], [9]–[11], they used MEMS oscillators for static displacement and showed a perfect ringing and settling-time reduction. For a high Q system, when a step input is applied, the system overshoots to twice the final rest position and then oscillates about that final rest position until it finally converges to that point. If instead, a half-step is applied, one half a period later, the system is at a peak of its excursion with an amplitude equal to the desired final rest position with a zero slope in the time history corresponding to zero velocity.

For nonlinear input/output micro-systems such as micro-mirrors and cantilevered parallel-plate actuators, zero-velocity and zero-velocity-and-derivative fail to function properly. To address this issue, a nonlinear command-shaping scheme was presented for electromagnetic actuators [14], [15], however, neglecting the effect of damping undermines the effectiveness of this method. Another nonlinear scheme was offered for command-shaping in an electrostatic torsional micro-mirror [13]. The results were satisfying concerning the settling time and handling the nonlinearities, however, nonlinear schemes were very complicated compared to the linear schemes and required an accurate knowledge of the nonlinear input/output relationship, which itself demanded a perplexing experimental and simulation process.

The most well-known actuation process in MEMS systems is the gap-closing (parallel-plate) configuration where an electrical potential between a movable electrode and a fixed electrode results in a mechanical motion. Beside the powerful features of MEMS parallel-plate configuration such as low energy requirements, there are some shortcomings that significantly limit their functionality. The parallel-plate configuration mostly suffers from the small range of motion as there is only a small gap between the electrodes and only one third of the initial gap is usable due to the pull-in instability. One may plan to increase the initial gap to solve this problem. Unfortunately, the initial gap cannot be too large because the effect of parallel-plate capacitive force is reduced drastically with the gap demanding a high voltage consumption.

We presented levitation-based MEMS actuators [18] to address the drawbacks with parallel-plate actuator and offered long range operation [20], and linear input/output relationship [17]. Building on linear actuator that we introduced, we show how open-loop control can be applied to provide significantly larger range of motion using electrostatic levitation compared to conventional gap-closing scheme. A micro-cantilever beam is actuated simultaneously by the gap-closing mechanism and levitating force mechanisms. The introduction is followed by a mechanism description and experimental setup (Section II) where the necessary procedures and the apparatus for conducting the tests are introduced. Experimental results are discussed in Section III. The results are then concluded in Section IV.

978-1-7281-9501-8/21/$31.00 ©2021 IEEE

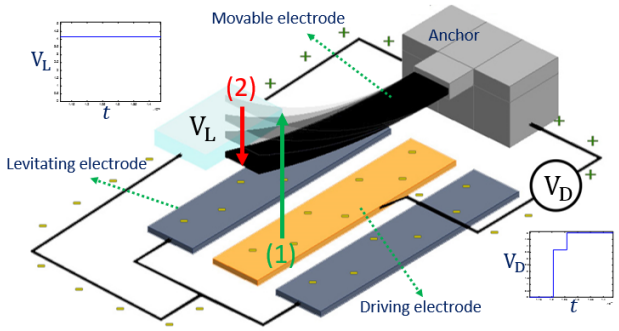

Fig. 1. Schematic of open-loop control of levitation-based MEMS. (1) shows the levitation of the micro-cantilever using the levitating electrodes. (2) shows the command-shaping driving part using the driving electrode.

Parameter	Symbol
Value	
Beam Length	$505\ \mu m$
Beam Width	$20.5\ \mu m$
Beam Thickness	$2\ \mu m$
Module of Elasticity	$160\ GPa$
Density	$2330\ kg/m^3$
Initial Gap	$2\ \mu m$
Driving electrode width	$32\ \mu m$
Levitating electrode width	$28\ \mu m$
Electrode Thickness	$0.5\ \mu m$

TABLE I
LEVITATION-BASED MEMS PARAMETERS AND PROPERTIES.

II. Experimental Setup and Open-Loop Control

The levitation-based MEMS system consists of a micro-cantilever as a movable electrode fabricated at $2\ \mu m$ above the substrate. Parallel to the movable electrode, a driving electrode was fabricated on the substrate. In addition, two electrodes were fabricated at each of the driving electrode which are responsible for applying levitating force to the movable electrode. Table I contains the parameters and properties of the system. The levitation-based MEMS was fabricated by MEMSCAP following the PolyMUMPS standard [16]. A Polytec MSA-500 laser vibrometer was used for displacement measurement of the micro-cantilever tip. Through a data acquisition system (National Instruments USB 6366 DAQ), the measurement data is transferred to MATLAB software. The driving-electrode receives the driving voltage by the same data acquisition system. Considering the large voltage required for the levitating electrodes, the command signal is firstly manipulated in MATLAB and then, it is sent to a wide-band amplifier, Krohn-Hite 7600. The amplified signal (V_L) charges the levitating electrodes. The tests were conducted in MEMS and Energy Harvesting Laboratory [19] in 22^oC and relative humidity of 37 %. To obtain the quality factor, the damping ratio including structural and air damping was determined using the experimental results. Using logarithmic decrement method, the damping ratio is measured as $\xi = 0.0025$ at air pressure of $P = 400\ mTorr$. The quality factor is obtained as

$$Q = \frac{1}{2\xi} = 200 \tag{1}$$

III. Results and Discussion

In this section, the open-loop control performance applied to a levitation actuator mechanism is demonstrated and discussed. As reported in one of our group publication [17], the electrostatic force can be obtained as a function of the gap between electrodes, the levitating voltage and the driving voltage using COMSOL simulation. The behavior of the system was characterized in the presence of constant levitating and driving voltages in our earlier work [20]. The driving force resembles the well-known parallel-plate electrostatic force, which increases drastically when the movable and the driving electrodes get closer to each other. For larger displacements in the range of one sixth of the initial gap, the driving force becomes weaker and mostly insensitive to the gap the maximum slope of $2.4 \times 10^{-8} N/per micron$. The levitating force varies slightly with the gap where the maximum slope of $5\ \times 10^{-9} N/per\ micron$ is observed beyond $4\mu m$ displacement. The small slope indicates that the electrostatic force can be considered as a constant force in the system dynamic equation which is a desirable feature for applying control methods such as double-step command-shaping of linear systems [11]. As shown in Fig. 2, the static displacement of the movable electrode is plotted versus the square of the driving voltage V_D. The results show that with $V_L = 120\ V$, the operation range is 7 times larger than the parallel-plate mechanism without levitating force. The graphs indicate the linear operation range where the driving force is a linear function of V_D^2 as:

$$Driving\ force = CV_D^2 \tag{2}$$

where C is approximated as a constant coefficient because as mentioned, when the displacement of the movable electrode is smaller than one sixth of the initial gap between the parallel plates. Fig. 2 also shows the range of motion in the linear regions is extended in the presence of larger levitating voltage V_L. Table II contains the achievable operation range and the signal-to-noise ratio using different levitating voltages. The signal-to-noise ratio is defined as:

$$Signal\text{-}to\text{-}noise\text{-}ratio = \frac{Linear\ operation\ range}{Uncontrolled\ ringing\ amplitude} \tag{3}$$

The uncontrolled ringing amplitude is the obtained from experimental results by subtracting the overshoot from the desired displacement. The linear operation range in Eq. (3) refers to the region that we can consider the driving force as a constant with respect to the system state. The signal-to-noise-ratio doubles by increasing the levitating voltage from 0 to 120 V.

For obtaining the time where the second step applies, we use procedure explained in [11]. The measurement of $f_0 = 9260$ Hz was observed for the fundamental frequency of the movable electrode. Using the time-response of a linear second-order system actuated by a single step, the movable electrode starts oscillating with the fundamental frequency. For reaching 96 % of the final displacement, we have to wait for t_1 as

Levitating Voltage	Operation Range	Signal to noise ratio
$V_L = 0\,V$	$0.36\,\mu m$	22.22
$V_L = 60\,V$	$0.85\,\mu m$	26.40
$V_L = 80\,V$	$1.11\,\mu m$	44.40
$V_L = 100\,V$	$1.95\,\mu m$	38.54
$V_L = 120\,V$	$2.48\,\mu m$	54.27

TABLE II
PERFORMANCE OF A LEVITATION MEMS ACTUATOR IN DOUBLE-STEP OPEN-LOOP CONTROL.

$$1 - 0.96 = e^{-2\pi f_0 \xi t_1} \tag{4}$$

Substituting Eq. (1) in Eq. (4), number of oscillations experienced during the settling time is obtained as

$$N = \frac{-ln(1-0.96)}{\pi} Q \approx 205\, oscillations \tag{5}$$

Using the double-step open-loop control reduces the settling time to half of the period, and as a result, the settling time is approximately reduced 410 times. The open-loop control operation in Fig. 3a demonstrates the driving voltage V_D (left axis) and the displacement $\delta(t)$ (right axis) versus time. For the desired displacement of $\delta_0 = 0.5\,\mu m$, the levitating voltages of $V_L = 60$ V, $V_L = 80$ V and $V_L = 100$ V accompanied with their corresponding driving voltages provide the appropriate range of motion. Compared to the single step command where the overshoot is twice the desired displacement, the ring-down amplitude has been significantly reduced by the open-loop control. Three more tests were conducted for the desired displacement of $1\,\mu m$ (Fig. 3b), which is possible using $V_L > 75\,V$. Similar results in ring-down and settling-time reduction were observed with the levitating voltages of $V_L = 80$ V, $V_L = 100$ V and $V_L = 120$ V. The stroke improvement is considerable as the travel range of $1\,\mu m$ micron is 2.5 times larger than the maximum allowable displacement of $0.4\,\mu\,m$ with no levitating voltage.

The electrostatic force of the parallel-plate mechanism is considered as a nonlinear force because of the dependence on the system state unless the electrode distance is sufficiently large. Electrostatic levitation creates a larger gap in the parallel-plate system and results in a linear region where the electrostatic force is only a function of the driving voltage not the gap. This unique feature enables the use of double-step command-shaping of linear systems which requires simple calculation as reported in [11].

IV. CONCLUSION

Compared to the parallel-plate, levitating the movable electrode by 4.5 microns results in a 5-time increase in the operation range and a significant increase of signal to noise ratio. Levitating the movable electrode in parallel-plate mechanism causes a large gap between the parallel electrodes which results in a linear input/output relation in a wider range. This enables using simpler command-shaping techniques such as linear double-step method instead of complicated nonlinear methods. The improvement of the operation range and linearity

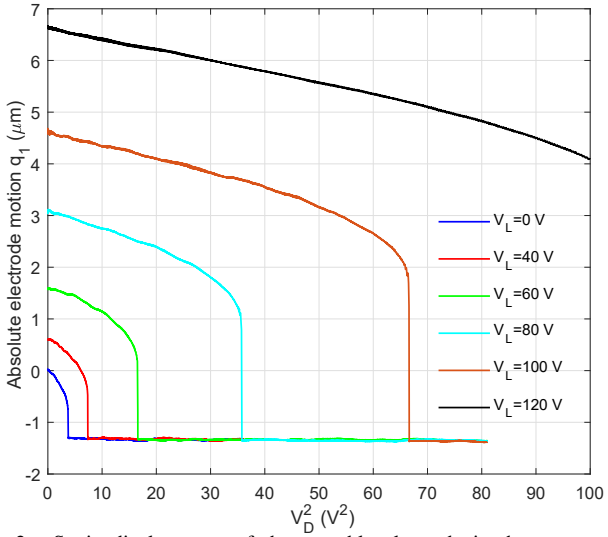

Fig. 2. Static displacement of the movable electrode in the presence of different levitating voltages. The linear regions are indicated where the motion is a function of square of the driving voltage V_D only.

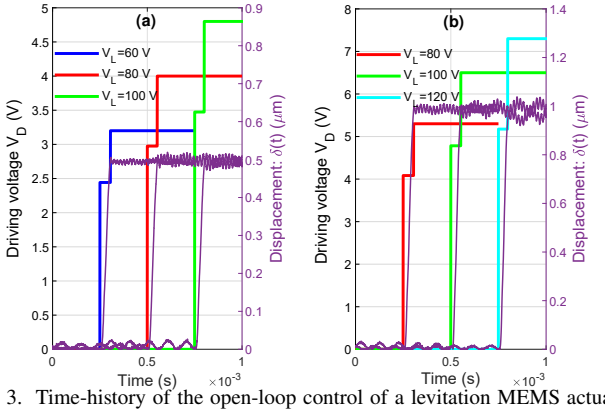

Fig. 3. Time-history of the open-loop control of a levitation MEMS actuator using double-step command-shaping in the presence of different levitating voltages. The double-step signals belong to the left axis which represents the driving voltage V_D. The purple signals represent the displacement of the movable electrode (right axis) corresponding to the driving voltage above each. (a) and (b) refer to the desired displacements of 0.5 and 1 micron, respectively.

in the open-loop control of MEMS actuators is obtained at the expense of providing an extra input voltage for the levitating mechanism.

ACKNOWLEDGMENT

The authors would like to acknowledge National Science Foundation (NSF) for the financial support of this study through grant CMMI 1919608.

REFERENCES

[1] D J. Bell,T J. Dominik, N A. Fleck and S M. Spearing, "MEMS actuators and sensors: observations on their performance and selection for purpose," *Journal of Micromechanics and Microengineering*, vol. 15, no. 7, p. S153, 2005.

[2] Ch. Liu, "Foundations of MEMS," *Pearson Education India*, 2012.

[3] M K. Mishra, V. Dubey, P M. Mishra and I. Khan, "MEMS technology: A review," *Journal of Engineering Research and Reports*, vol. 4, no. 1, p. 1-24, 2019.

[4] Sh Ch. Chen, V. Dubey, M. Culpepper and L. Martin, "Design of a six-axis micro-scale nanopositioner—μHexFlex," *Precision engineering*, vol. 30, no. 3, p. 314-324, 2006.

[5] M. Imboden, H. Han, P. Jackson, B. Flavio, A. Cristian, E. Lowell, and D J. Bishop,"Atomic calligraphy: The direct writing of nanoscale structures using a microelectromechanical system," *Nano letters*, vol. 13, no. 7, p. 3379-3384, 2013.

[6] L K. Barrett, T. Stark, J. Reeves, A. Cristian, R. Lally, A. Stange, C. Pollock and, M. Imboden, and D J. Bishop,"A large range of motion 3D MEMS scanner with five degrees of freedom," *Journal of Microelectromechanical Systems*, vol. 28, no. 1, p. 170-179, 2019.

[7] C. Pollock, J. Javor, A. Stange, L K. Barrett, and D J. Bishop,"Extreme angle, tip-tilt MEMS micromirror enabling full hemispheric, quasi-static optical coverage," *Optics express*, vol. 27, no. 11, p. 15318-15326, 2019.

[8] Sh Ch. Chen, M L. Culpepper, S. Jordan, C. Scott, J. Danieli, and J. Wenger,"Application of input shaping and hyperBit control to improve the dynamic performance of a six-axis MEMS nano-positioner," *ASPE*, 2006.

[9] C. Pollock, L K. Barrett, P G. del Corro, A. Stange, and D J. Bishop,"PWM as a low cost method for the analog control of MEMS devices," *Journal of Microelectromechanical Systems*, vol. 28, no. 2, p. 245-253, 2019.

[10] C. Pollock, M. Imboden, A. Stange, J. Javor, K. Mahapatra, L. Chiles, D J. Bishop,"Engineered PWM drives for achieving rapid step and settle times for MEMS actuation," *Journal of Microelectromechanical Systems*, vol. 27, no. 3, p. 513-520, 2018.

[11] M. Imboden, J. Chang, C. Pollock, E. Lowell, M. Akbulut, J. Morrison, T. Stark, T G. Bifano, and D J. Bishop"High-speed control of electromechanical transduction: Advanced drive techniques for optimized step-and-settle response of MEMS micromirrors," *IEEE Control Systems Magazine*, vol. 36, no. 5, p. 48-76, 2016.

[12] V. Milanović, K. Castelino, C. Pollock, E. Lowell, M. Akbulut, J. Morrison, T. Stark, T G. Bifano, and D J. Bishop"Sub-100 μs settling time and low voltage operation for gimbal-less two-axis scanners," *IEEE/LEOS Optical MEMS*, vol. 36, no. 5, p. 48-76, 2016.

[13] W. P. Eaton and J. H. Smith, "Multistep-shaping control based on the static and dynamic behavior of nonlinear optical torsional micromirror," *Optical Engineering*, vol. 53, no. 5, p. 057109, 2014.

[14] K. Chen, T. Yang, and J. Yin, "Residual vibration suppression for duffing nonlinear systems with electromagnetical actuation using nonlinear command shaping techniques," *Journal of Vibration and Acoustics*, vol. 128, no. 6, p. 778-789, 2006.

[15] K. Chen, and K. Ou, "Command-shaping techniques for electrostatic MEMS actuation: Analysis and simulation," *Journal of microelectromechanical systems*, vol. 16, no. 3, p. 537-549, 2007.

[16] A. Cowen, B. Hardy, R. Mahadevan, and S. Wilcenski, "PolyMUMPs Design Handbook a MUMPs® process," *http://www.memscap.com/__data/assets/pdf_file/0019/1729/PolyMUMPs-DR-13-0.pdf*, 2011.

[17] M. Pallay, R. Miles, and S. Towfighian, "Merging parallel-plate and levitation actuators to enable linearity and tunability in electrostatic MEMS," *Journal of Applied Physics*, vol. 126, no. 1, p. 014501, 2019.

[18] M. Pallay, M. Daeichin, and S. Towfighian "Dynamic behavior of an electrostatic MEMS resonator with repulsive actuation", *Nonlinear Dynamics*, Vol. 89, no. 2, pp. 1525-1538, 2017.

[19] "MEMS and Energy Harvesting Laboratory," *https://www.binghamton.edu/labs/mems/*

[20] M. Mousavi, M. Alzgool, and S. Towfighian, "Electrostatic levitation: an elegant method to control MEMS switching operation," *Nonlinear Dynamics*, vol. 104, p. 3139–3155, 2021.